

# Dominance of particulate organic carbon in top mineral soils in cold regions

Received: 28 March 2023

Accepted: 30 November 2023

Published online: 04 January 2024

 Check for updates

Pablo García-Palacios  <sup>1,2</sup>✉, Mark A. Bradford  <sup>3</sup>, Iria Benavente-Ferraces  <sup>1</sup>, Miguel de Celis  <sup>1</sup>, Manuel Delgado-Baquerizo  <sup>4</sup>, Juan Carlos García-Gil  <sup>1</sup>, Juan J. Gaitán  <sup>5,6,7</sup>, Asier Goñi-Urtiaga <sup>1</sup>, Carsten W. Mueller  <sup>8</sup>, Marco Panettieri  <sup>1</sup>, Ana Rey  <sup>9</sup>, Tadeo Sáez-Sandino  <sup>10</sup>, Edward A. G. Schuur  <sup>11</sup>, Noah W. Sokol  <sup>12</sup>, Leho Tedersoo  <sup>13,14</sup> & César Plaza  <sup>1</sup>

The largest stocks of soil organic carbon can be found in cold regions such as Arctic, subarctic and alpine biomes, which are warming faster than the global average. Discriminating between particulate and mineral-associated organic carbon can constrain the uncertainty of projected changes in global soil organic carbon stocks. Yet carbon fractions are not considered when assessing the contribution of cold regions to land carbon–climate feedbacks. Here we synthesize field paired observations of particulate and mineral-associated organic carbon in the mineral layer, along with experimental warming data, to investigate whether the particulate fraction dominates in cold regions and whether this relates to higher soil organic carbon losses with warming than in other (milder) biomes. We show that soil organic carbon in the first 30 cm of mineral soil is dominated or co-dominated by particulate carbon in both permafrost and non-permafrost soils, and in Arctic and alpine ecosystems but not in subarctic environments. Our findings indicate that soil organic carbon is most vulnerable to warming in cold regions compared with milder biomes, with this vulnerability mediated by higher warming-induced losses of particulate carbon. The massive soil carbon accumulation in cold regions appears distributed predominantly in the more vulnerable particulate fraction rather than in the more persistent mineral-associated fraction, supporting the likelihood of a strong, positive land carbon–climate feedback.

Soil organic carbon (SOC) accumulates in cold regions such as Arctic, subarctic and alpine environments<sup>1</sup>. Approximately 37% of the global SOC stock, down to a depth of two metres, is stored in these cold regions<sup>2,3</sup>, and this vast SOC store is increasingly at risk under climate

warming because of the alleviation of temperature limitation for microbial decay<sup>4,5</sup>. Furthermore, the large SOC stocks in cold regions are not only inherently more temperature sensitive than those in warmer environments<sup>6,7</sup>, but also will be subjected to two to four times higher

<sup>1</sup>Instituto de Ciencias Agrarias (ICA), CSIC, Madrid, Spain. <sup>2</sup>Department of Plant and Microbial Biology, University of Zurich, Zurich, Switzerland.

<sup>3</sup>The Forest School, Yale School of the Environment, Yale University, New Haven, CT, USA. <sup>4</sup>Laboratorio de Biodiversidad y Funcionamiento Ecosistémico.

Instituto de Recursos Naturales y Agrobiología de Sevilla (IRNAS), CSIC, Seville, Spain. <sup>5</sup>National Institute of Agricultural Technology (INTA), Institute of Soil Science, Hurlingham, Argentina.

<sup>6</sup>Department of Technology, National University of Luján, Luján, Argentina. <sup>7</sup>National Research Council of Argentina (CONICET), Buenos Aires, Argentina.

<sup>8</sup>Department of Geosciences and Natural Resource Management, University of Copenhagen, Copenhagen, Denmark. <sup>9</sup>Museo Nacional de Ciencias Naturales (MNCN), CSIC, Madrid, Spain. <sup>10</sup>Departamento de Sistemas Físicos, Químicos y Naturales, Universidad Pablo de Olavide, Seville, Spain.

<sup>11</sup>Center for Ecosystem Society and Science, Northern Arizona University, Flagstaff, AZ, USA. <sup>12</sup>Physical and Life Sciences Directorate, Lawrence Livermore National Laboratory, Livermore, CA, USA. <sup>13</sup>Mycology and Microbiology Center, University of Tartu, Tartu, Estonia.

<sup>14</sup>College of Science, King Saud University, Riyadh, Saudi Arabia. ✉e-mail: [pablo.garcia@ica.csic.es](mailto:pablo.garcia@ica.csic.es)

warming rates than the global average due to the Arctic amplification phenomenon<sup>8,9</sup>. Together, these factors set the scene for a dramatic release of C to the atmosphere from SOC stocks in cold regions that will accelerate anthropogenic global climate warming within a timescale of decades to centuries<sup>3,4</sup>.

Different fractions of SOC, which are found within the soil depending on the decomposition pathway of incoming organic matter combined with pedogenic processes, may not respond to global warming in a similar manner<sup>10,11</sup>. For example, particulate organic C (POC) may be more susceptible to warming-induced microbial decomposition than mineral-associated organic C (MAOC) since POC is not occluded in micropores or microaggregates and/or bound to mineral surfaces, all of which limit microbial accessibility in the MAOC fraction<sup>12–14</sup>. Despite the importance of SOC in cold regions for the land C-climate feedback<sup>4,15</sup>, no global studies have investigated the dominance of different SOC fractions in these areas. An effort to compare POC versus MAOC proportions in cold ecosystems, mirroring those conducted for tropical and temperate biomes<sup>11,16</sup>, will inform whether the fraction composition of SOC points towards a reinforcing or limiting of the land C feedback to climate change from these regions.

A number of features may determine the dominance of POC versus MAOC in cold regions, influencing the mechanisms that control SOC persistence and turnover. In permafrost soils, the ground remaining below 0 °C for at least two consecutive years<sup>17</sup>, extremely low temperatures, freeze-thaw dynamics and water availability and saturated soils are major controls of SOC dynamics<sup>4</sup> and fraction dominance<sup>18,19</sup> compared with non-permafrost soils. Carbon distribution in POC and MAOC can also differ across Arctic, subarctic and alpine biomes as a range of plant and microbial traits, climatic conditions and soil mineralogy play contrasting roles as controls on fraction C concentrations across biome types<sup>11,16,20</sup>. Soil depth may also be important as the effects of surface cryoturbation in thermokarst-impacted landscapes can increase C association with reactive iron minerals<sup>18,21</sup>, forming MAOC over POC. Despite these known differences, the distribution of SOC across different fractions, biomes, permafrost and non-permafrost soils and soil depths remains elusive.

We assessed the distribution of SOC in the POC and MAOC fractions in the mineral layer of cold regions located in the Northern Hemisphere. Our global literature survey included 134 (the first 30 cm of mineral soil) and 28 (>30 cm depth) paired POC and MAOC observations from Arctic (57), subarctic (41) and alpine (64) biomes (Extended Data Fig. 1). We first addressed whether C in cold regions is stored predominantly in the POC or the MAOC fractions and whether this dominance changes across soil depths, permafrost and non-permafrost soils and biome types. Then we evaluated potential environmental controls (climate, soil properties, active layer thickness and net primary productivity) on the C stored in the POC versus MAOC fractions. Last, we collected data from field sites that experimentally manipulated ambient temperatures and tested whether climate warming drives SOC losses via changes in primarily the POC or the MAOC fractions in cold regions (18 observations) compared with other (milder) biomes (22 observations). If C in the top mineral layer is stored predominantly as POC, probably triggering higher relative SOC losses with warming compared with milder biomes, then such a result would build evidence for a potentially dramatic land C-climate feedback involving Earth's cold-region soils.

## Results

### POC dominates or co-dominates in cold regions

Overall, we found that POC concentration in the top mineral layer (median: 19.7 gC kg<sup>-1</sup>; interquartile range: 38.5) was 40% higher than in the MAOC fraction (median: 14.1 gC kg<sup>-1</sup>; interquartile range: 18.7; Fig. 1a). This pattern was confirmed when controlling for multiple environmental drivers by linear mixed-effects modelling (Extended Data Fig. 2). The dominance of POC over MAOC was most evident when considering

only the observations using the particle-size fractionation method, but POC still co-dominated with MAOC when using density methods (Extended Data Fig. 3). The higher abundance of POC over MAOC was restricted to the first 30 cm of mineral soil; there was no difference between POC and MAOC in the >30 cm layer (Fig. 1b and Extended Data Fig. 2). The larger concentration of POC relative to MAOC in the first 30 cm of mineral soil was of greater magnitude in permafrost-affected soils than in non-permafrost soils (Fig. 1c and Extended Data Fig. 2), with 75% and 68% increases in the corresponding medians, respectively. At the biome level, POC was significantly greater than MAOC concentration in the first 30 cm of mineral soil in Arctic and alpine sites but not in the subarctic sites (Fig. 1d). Both fractions increased with SOC (Fig. 2), but the slope was steeper for POC (slope: 0.66;  $P < 0.001$ ) than for MAOC (slope: 0.34;  $P < 0.001$ ). As a consequence, POC became more dominant relative to MAOC as SOC concentration increased.

### Different environmental drivers of POC and MAOC

Separate linear mixed-effects models for each C fraction (Fig. 3) indicated that POC and MAOC in the top mineral layer were negatively associated with mean annual temperature (MAT) (estimate (POC): -0.29, 95% confidence interval (CI): -0.84 to 0.29; estimate (MAOC): -0.72, 95% CI: -1.20 to -0.24), but positively associated with mean annual precipitation (MAP) (estimate (POC): 0.49, 95% CI: -0.04 to 0.99; estimate (MAOC): 0.75, 95% CI: 0.33 to 1.18). Net primary productivity (NPP) increased POC (estimate: 0.61, 95% CI: 0.15 to 1.08) but did not affect MAOC. We also found a positive association between both C fractions and soil clay-and-silt content (estimate (POC): 0.65, 95% CI: 0.22 to 1.11; estimate (MAOC): 0.55, 95% CI: 0.18 to 0.93). To build confidence in our conclusions from this analysis of our observational dataset, we also addressed the relative importance of the environmental drivers using random forests modelling. We found that the most important predictors of POC (NPP and soil clay and silt) and MAOC (MAT and soil clay and silt) in the random forests models (Extended Data Fig. 4) were also significant predictors in the linear mixed-effects models (Fig. 3).

### POC is vulnerable to experimental warming

There was a tendency for decreased SOC with warming in the top mineral layer of cold regions (mean percentage change (MPC): -15.46%; CI: -30.16 to 2.33; Fig. 4 and Extended Data Table 1) but not in the other biomes' category (MPC: -0.30%; CI: -13.15 to 14.45). In line with this result, we found a significant negative effect of warming on POC in cold regions (MPC: -27.89%; CI: -47.48 to -0.90) but not in other biomes (MPC: 17.00%; CI: -4.40 to 43.33). The results of the meta-regression confirmed the differential effects of warming on POC in cold regions compared with other biomes as biome type was a significant moderator ( $P = 0.008$ ). MAOC did not respond to warming in either cold regions or other biomes.

## Discussion

Soils represent the largest actively cycling pool of C in terrestrial ecosystems, holding more C than plants and the atmosphere combined<sup>2,22</sup>. Cold regions such as Arctic, subarctic and alpine environments store a massive SOC stock that is being released to the atmosphere under anthropogenic global warming, intensifying climate change<sup>5,15</sup>. The mineral protection of soil organic matter (the formation of MAOC) has been proposed as a fundamental mechanism controlling the long-term persistence of SOC<sup>10,23</sup>. Our observational analysis demonstrates that SOC in the top mineral layer of cold regions (the first 30 cm of mineral soil) is dominated on average, however, not by MAOC but by the POC fraction, in both permafrost and non-permafrost soils, as well as in Arctic and alpine ecosystems (although not in subarctic environments). The synthesis of experimental warming studies suggests that SOC is more vulnerable to warming in cold ecosystems compared with milder biomes, given higher warming-induced POC losses. Not only

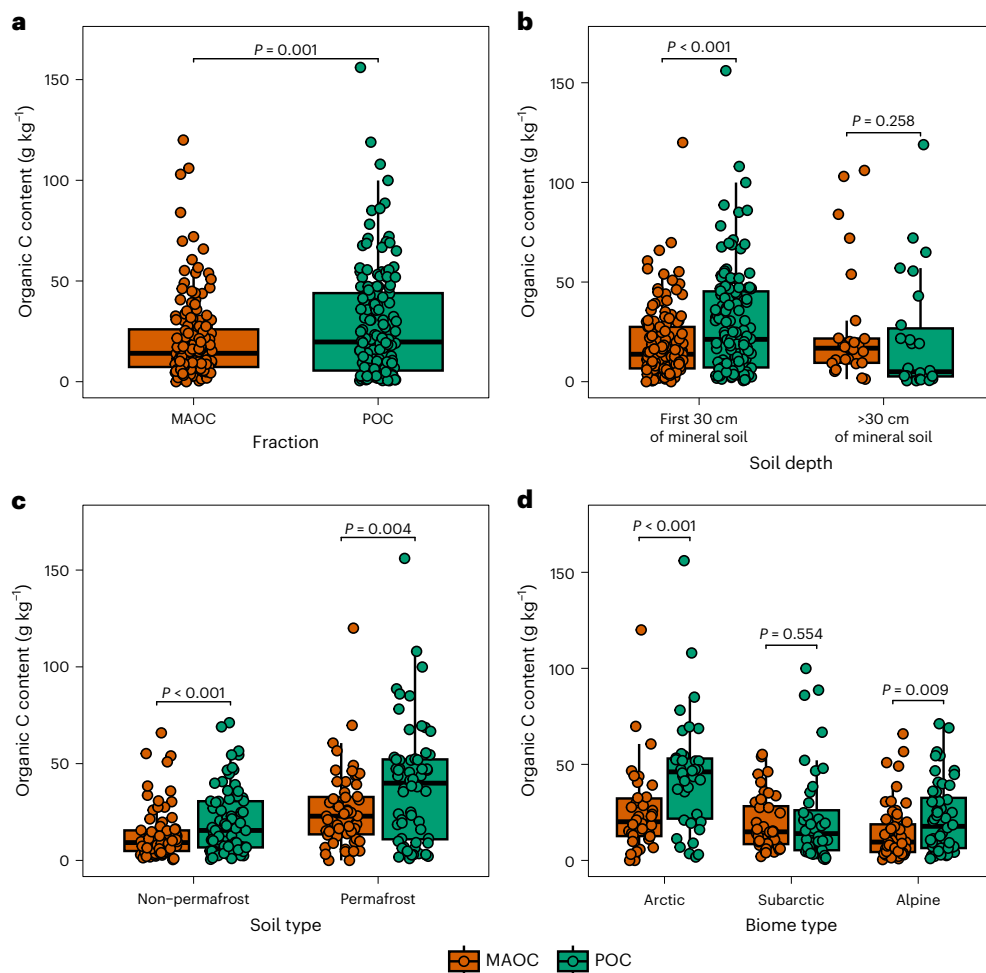


**Fig. 1 | Distribution of SOC in the POC and MAOC fractions in the mineral layer of cold regions.** **a–d**, Overall fraction distribution ( $n = 159$  for both fractions) (a) or separated by soil depth (the first 30 cm of mineral soil ( $n = 133$ ) and  $>30$  cm ( $n = 26$ )) (b), permafrost ( $n = 59$ ) versus non-permafrost soils ( $n = 74$ ) (c) and biome type (Arctic ( $n = 38$ ), subarctic ( $n = 40$ ) and alpine ( $n = 55$ ))

(d). Results from paired Wilcoxon signed-rank tests. Data in c,d correspond to the first 30 cm of mineral soil. Box plots represent first and third quartiles (box), medians (central horizontal line), largest value smaller than 1.5 times the interquartile range (upper vertical line) and smallest value larger than 1.5 times the interquartile range (lower vertical line).  $P$  values for two-tailed tests.

are the large SOC stocks in cold regions subjected to a higher degree of warming than the global average<sup>8</sup>, but proportionally more of the SOC is stored in the POC fraction—the fraction most vulnerable to anthropogenic climate warming.

The relationship between soil C inputs and outputs balances the global SOC stock on an annual basis<sup>24</sup>. However, climate warming may destabilize this balance because microbial-mediated SOC losses under warming are expected to increase more than soil C inputs from plant residues<sup>5</sup>. The net outcome of these warming effects is uncertain in cold regions<sup>25</sup>, but the relative dominance of POC over MAOC found may point towards higher SOC losses than expected due to faster C turnover in these cold environments. Such an effect may be particularly conspicuous under high-emissions scenarios, where gains in vegetation C are not large enough to compensate for SOC losses<sup>26</sup>. In permafrost-affected soils, POC dominates or co-dominates (Fig. 1c), which may render the total SOC pool more susceptible to rapid microbial breakdown upon permafrost thaw<sup>27,28</sup>. These results are relevant at the global scale because the permafrost C-climate feedback has been projected to account for 0.27 °C additional global warming by 2100 and up to 0.42 °C by 2300 in high-emissions scenarios<sup>4,25</sup>. The representation of SOC fractions in biogeochemical models may help to constrain the uncertainty of projected change in global SOC estimates<sup>18</sup>, as has been demonstrated in other global biomes<sup>16</sup>.

The potential for large SOC losses under warming as a result of high POC concentrations may be modulated because the concentration of MAOC in permafrost soils may shift under climate change. For example, warming-induced increases in iron-bound organic C have been found on a permafrost-thaw sequence on the Qinghai-Tibet Plateau<sup>18</sup>. Thus, alongside the initial C release from the microbial decomposition of the POC fraction, an increase in the stability of the MAOC fraction may dampen the gradual permafrost C-climate feedback over decades or centuries—the timescale where these feedbacks are more likely to cause abrupt climate change<sup>4</sup>. In our study, we used the increase in the active layer thickness as a surrogate of warming-induced permafrost thaw, which is commonly used in permafrost modelling<sup>29,30</sup>. Interestingly, the increased thickness of the active layer is associated with a higher relative dominance of MAOC over POC in the total SOC (fMAOC, Pearson's  $r = 0.29$ ,  $P = 0.03$ ; Extended Data Fig. 5). However, waterlogging and oxygen limitation across a spatial gradient of permafrost thaw have also been found to induce the dissolution of iron minerals and release of MAOC in the Arctic permafrost<sup>31</sup>. Therefore, whether changes in the stability of MAOC upon long-term permafrost thaw can alleviate POC losses with warming remains a critical issue to constrain the land C-climate feedback from cold regions. To address this unknown, direct evaluations of thaw dynamics at sentinel sites may help to overcome the limitations of space for time approaches.

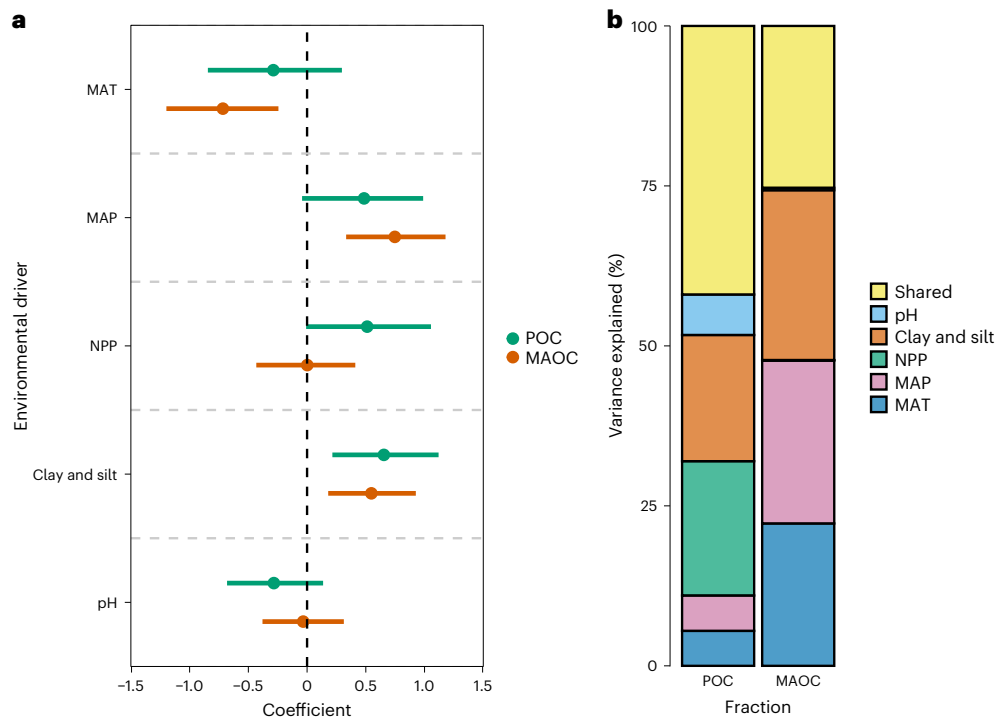
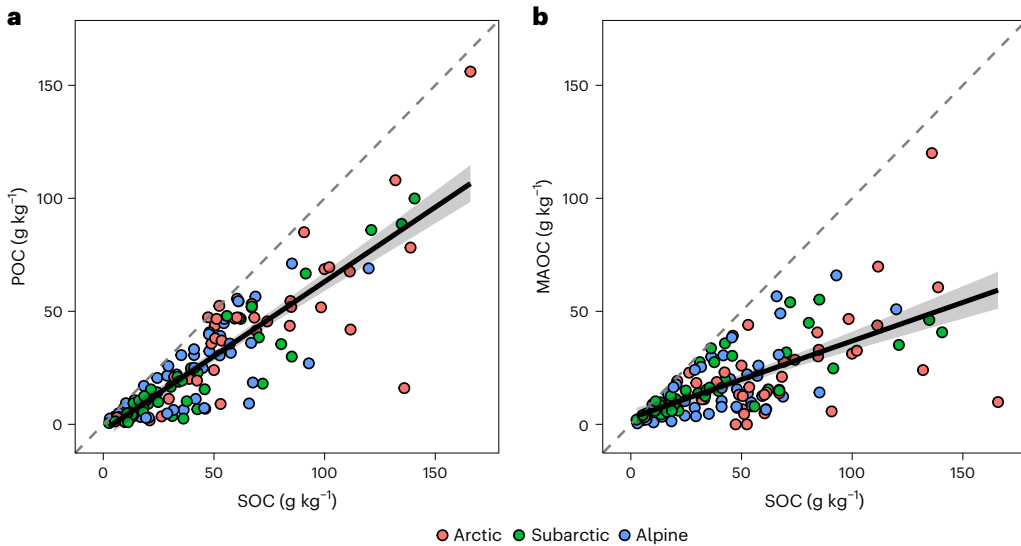


**Fig. 3 | Effects of environmental drivers on POC and MAOC concentrations in the top mineral layer (first 30 cm) of cold regions.** **a**, The coefficients (dots) and 95% CIs (lines) of the fixed effects of MAT ( $P = 0.334$  for POC and  $P = 0.004$  for MAOC), MAP ( $P = 0.061$  for POC and  $P < 0.001$  for MAOC), NPP ( $P = 0.066$  for POC and  $P = 0.995$  for MAOC), soil clay-and-silt content ( $P = 0.005$  for POC and  $P = 0.005$  for MAOC) and soil pH ( $P = 0.170$  for POC and  $P = 0.856$  for MAOC) from a linear mixed-effects model ( $P$  values for two-tailed tests).

**b**, The percentage of the variance explained by the fixed effects uniquely attributable to each predictor and shared among them. The variance explained by the fixed-effects predictors and random effects relative to the total variance ( $R^2$ ) was 30% and 36%, respectively, for POC ( $n = 128$ ) and 29% and 14%, respectively, for MAOC ( $n = 127$ ). POC and MAOC concentrations were natural-log transformed.

The dominance of POC over MAOC is more evident when considering the size fractionation studies only, which encompass a larger number of observations across a wider biome distribution than density studies (Extended Data Fig. 3). However, studies using density methods still reveal co-dominance of POC with MAOC, as opposed to the MAOC dominance expected from work in temperate and tropical biomes<sup>11,12</sup>. Overall, the consideration of both physical fractionation methods in our analysis contributes to a more conservative assessment of POC

contributions to total SOC, as performed for other terrestrial ecosystems<sup>11,16,32</sup>. Our quantitative synthesis also demonstrates that whereas SOC in the first 30 cm of mineral soil is dominated largely by POC, the pattern is not found at deeper soil layers (>30 cm). The ubiquity of this finding is uncertain because the number of studies including subsoil data was lower compared with topsoils. The assessment of SOC from cold systems at deep soil layers such as in Yedoma deposits remains a priority for soil C research, and we further advocate including POC

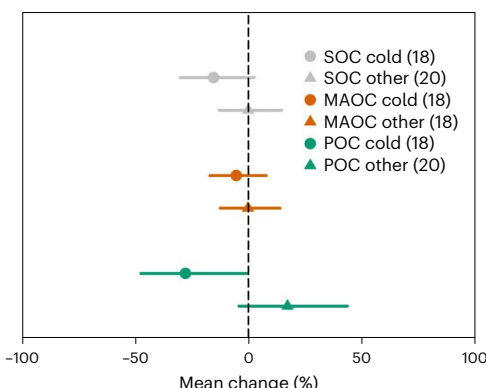


**Fig. 4 | Mean effect size of experimental warming on SOC, POC and MAOC in the top mineral layer (first 30 cm) of cold systems versus other biomes.** Lines around symbols (log response ratios) are 95% CIs.

and MAOC fractions in such efforts to improve the prediction of SOC vulnerability to climate warming.

Our results further indicate that in Arctic and alpine biomes, POC dominates or co-dominates SOC in the top 30 cm of mineral soil. The large accumulations of undecomposed plant residues in the organic horizon and excess soil moisture may be the precursor to the higher POC observed in the Arctic and in swamp meadows of the Tibetan plateau<sup>33,34</sup>, although other mechanisms may operate in drier alpine steppes. In addition, the reactivity of soil minerals is very low under the permafrost conditions in these areas<sup>35</sup>, while the portion of undecomposed soil organic matter with reduced functional groups is high, which limits the occurrence of organo–mineral interactions<sup>23</sup>. In contrast to MAOC, C accumulation in the POC fraction is not dependent on a finite availability of mineral surfaces to interact with<sup>20</sup> and can, in theory, accumulate indefinitely if C inputs are not limiting. Such a dynamic appears consistent with the steeper slope of the SOC versus POC than the SOC versus MAOC relationship that was driven by higher POC concentrations at the Arctic sites (Fig. 2).

Concentrations of MAOC and POC in cold regions were associated with a set of distinct and overlapping environmental drivers, as confirmed by both linear mixed and random forest modelling (Fig. 3 and Extended Data Fig. 4). Whereas MAOC was linked mainly with climate and soil clay-and-silt content, POC was related to plant inputs (NPP) and soil clay-and-silt content. Higher MAOC concentrations were found at lower temperatures, highlighting the strong role of temperature limitation for persistence of the mineral-protected fraction. Soil clay-and-silt content positively affected both fractions, indicating that POC and MAOC are higher in clayey soils that host larger mineral surface area and reactive sites for C adsorption<sup>36,37</sup>. However, the lack of data on predictors in the studies included in the meta-analysis prevented us from addressing the contribution of other potentially important soil mineralogical variables for organo–mineral interactions, particularly the mineral type, the proportion of reactive minerals, their specific surface area and the availability of binding sites<sup>16</sup>. There was a positive relationship between POC and NPP, suggesting that, beyond potential effects of the build-up of relatively undecomposed plant material in the organic horizons<sup>18,38</sup>, increased plant C inputs probably also contribute to C accumulation in the POC fraction of the mineral layer. We call for future empirical studies addressing a full suite of biological, chemical and mineralogical soil properties to gain mechanistic insights into POC and MAOC distributions in cold regions.

Finally, we found more-pronounced SOC and POC losses from the mineral layer with experimental warming in cold regions than in other (milder) biomes (Fig. 4). These results confirmed the pattern found in a previous meta-analysis<sup>39</sup>, where POC losses with warming increased with latitude. Climate warming decreases the temperature limitation for

microbial decomposition of POC in cold ecosystems<sup>7,40</sup>, and this probably drives the greater POC and SOC losses. Conversely, POC increased with warming in other biomes, although this response was not significant. In these milder biomes, warming-induced increases in NPP are more likely to compensate or even outpace soil respiratory losses<sup>5</sup>, which are not as sensitive to temperature as in cold regions<sup>6,7</sup>. However, we caution that we evaluated only warming studies that reported fraction data, which markedly reduced the number of studies available for synthesis. The minimal mean change in total SOC under experimental warming in other biomes may then not be representative of broader patterns. As such, we suggest that the most valid interpretation of our findings is that SOC losses are probably relatively greater in cold biomes due to the sensitivity of POC decomposition to warming. Future empirical research needs to quantify C inputs from plant growth and C outputs from microbial decomposition and consider warming effects on the overlying organic horizon. In addition, the mechanisms behind POC losses with warming may be different in non-permafrost soils and in soils affected by gradual permafrost thaw, compared with soils suffering from abrupt thaw. In regions experiencing abrupt permafrost thaw, the mineral protection of SOC may be less efficient due to enhanced soil aeration<sup>41</sup> and increased lateral C transport through gullies and slumps in thermokarst-impacted sites<sup>42</sup>. Nevertheless, in the much larger permafrost areas experiencing more gradual thawing, and in non-permafrost soils, the size of POC probably exceeds the capacity of the soil mineral matrix to dampen losses of SOC from microbial decomposition under warming climates. The relative dominance of the POC fraction and its higher vulnerability to increased warming point towards a reinforcing of the land C feedback to climate change from cold regions.

## Conclusion

We observed that C in the top mineral layer of cold regions dominates or co-dominates on average in the POC fraction compared with the MAOC fraction. This pattern was found in permafrost-affected sites and in those sites without a permafrost layer, and in Arctic and alpine ecosystems but not in subarctic environments. Concentrations of MAOC and POC were associated with different sets of environmental drivers, with MAOC linked mainly with climate and soil parameters and POC with plant inputs and soil parameters. The dominance of POC agreed with the higher temperature vulnerability of SOC found in cold compared with milder biomes, as mediated by higher warming-induced POC losses in the former. Recent research and international initiatives have profoundly advanced our understanding of the contribution of SOC from cold regions to global climate regulation, from increased microbial breakdown of SOC with warming<sup>7</sup> to the quantification of SOC within deeper soil profiles<sup>34</sup> and the effects of permafrost-thaw timing (gradual versus abrupt)<sup>30</sup>. However, the emerging SOC fraction framework has not yet been integrated into such large spatiotemporal studies. Our study demonstrates the relative dominance of the POC fraction in cold regions, sets a critical baseline for understanding how the massive SOC stock in these areas will respond to climate change and builds evidence for a dramatic land C–climate feedback driven by Earth’s cold biomes.

## Online content

Any methods, additional references, Nature Portfolio reporting summaries, source data, extended data, supplementary information, acknowledgements, peer review information; details of author contributions and competing interests; and statements of data and code availability are available at <https://doi.org/10.1038/s41561-023-01354-5>.

## References

- Crowther, T. W. et al. The global soil community and its influence on biogeochemistry. *Science* **365**, eaav0550 (2019).
- Jackson, R. B. et al. The ecology of soil carbon: pools, vulnerabilities, and biotic and abiotic controls. *Annu. Rev. Ecol. Evol. Syst.* **48**, 419–445 (2017).

3. Schuur, E. A. G. et al. Permafrost and climate change: carbon cycle feedbacks from the warming arctic. *Annu. Rev. Environ. Resour.* **47**, 343–371 (2022).
4. Schuur, E. A. G. et al. Climate change and the permafrost carbon feedback. *Nature* **520**, 171–179 (2015).
5. García-Palacios, P. et al. Evidence for large microbial-mediated losses of soil carbon under anthropogenic warming. *Nat. Rev. Earth Environ.* **2**, 507–517 (2021).
6. Carey, J. C. et al. Temperature response of soil respiration largely unaltered with experimental warming. *Proc. Natl Acad. Sci. USA* **113**, 13797–13802 (2016).
7. Koven, C. D., Hugelius, G., Lawrence, D. M. & Wieder, W. R. Higher climatological temperature sensitivity of soil carbon in cold than warm climates. *Nat. Clim. Change* **7**, 817–822 (2017).
8. Rantanen, M. et al. The Arctic has warmed nearly four times faster than the globe since 1979. *Commun. Earth Environ.* **3**, 168 (2022).
9. Jansen, E. et al. Past perspectives on the present era of abrupt Arctic climate change. *Nat. Clim. Change* **10**, 714–721 (2020).
10. Lavallee, J. M., Soong, J. L. & Cotrufo, M. F. Conceptualizing soil organic matter into particulate and mineral-associated forms to address global change in the 21st century. *Glob. Change Biol.* **26**, 261–273 (2020).
11. Sokol, N. W. et al. Global distribution, formation and fate of mineral-associated soil organic matter under a changing climate: a trait-based perspective. *Funct. Ecol.* **36**, 1411–1429 (2022).
12. Benbi, D. K., Boparai, A. K. & Brar, K. Decomposition of particulate organic matter is more sensitive to temperature than the mineral associated organic matter. *Soil Biol. Biochem.* **70**, 183–192 (2014).
13. Lugato, E., Lavallee, J. M., Haddix, M. L., Panagos, P. & Cotrufo, M. F. Different climate sensitivity of particulate and mineral-associated soil organic matter. *Nat. Geosci.* **14**, 295–300 (2021).
14. Liu, X. J. A. et al. Soil aggregate-mediated microbial responses to long-term warming. *Soil Biol. Biochem.* **152**, 108055 (2021).
15. Zimov, S. A., Schuur, E. A. G. & Iii, F. S. C. Permafrost and the global carbon budget. *Science* **312**, 1612–1613 (2006).
16. Georgiou, K. et al. Global stocks and capacity of mineral-associated soil organic carbon. *Nat. Commun.* **13**, 3797 (2022).
17. Schuur, E. A. G. & MacK, M. C. Ecological response to permafrost thaw and consequences for local and global ecosystem services. *Annu. Rev. Ecol. Evol. Syst.* **49**, 279–301 (2018).
18. Liu, F. et al. Divergent changes in particulate and mineral-associated organic carbon upon permafrost thaw. *Nat. Commun.* **13**, 5073 (2022).
19. Gentsch, N. et al. Temperature response of permafrost soil carbon is attenuated by mineral protection. *Glob. Change Biol.* **24**, 3401–3415 (2018).
20. Cotrufo, M. F., Ranalli, M. G., Haddix, M. L., Six, J. & Lugato, E. Soil carbon storage informed by particulate and mineral-associated organic matter. *Nat. Geosci.* **12**, 989–994 (2019).
21. Joss, H. et al. Cryoturbation impacts iron–organic carbon associations along a permafrost soil chronosequence in northern Alaska. *Geoderma* **413**, 115738 (2022).
22. IPCC Climate Change 2021: The Physical Science Basis (eds Masson-Delmotte, V. et al.) (Cambridge Univ. Press, 2021).
23. Lehmann, J. & Kleber, M. The contentious nature of soil organic matter. *Nature* **528**, 60–68 (2015).
24. Davidson, E. A. & Janssens, I. A. Temperature sensitivity of soil carbon decomposition and feedbacks to climate change. *Nature* **440**, 165–173 (2006).
25. Burke, E. J. et al. Quantifying uncertainties of permafrost carbon-climate feedbacks. *Biogeosciences* **14**, 3051–3066 (2017).
26. McGuire, A. D. et al. Dependence of the evolution of carbon dynamics in the northern permafrost region on the trajectory of climate change. *Proc. Natl Acad. Sci. USA* **115**, 3882–3887 (2018).
27. Dutta, K., Schuur, E. A. G., Neff, J. C. & Zimov, S. A. Potential carbon release from permafrost soils of Northeastern Siberia. *Glob. Change Biol.* **12**, 2336–2351 (2006).
28. Elberling, B. et al. Long-term CO<sub>2</sub> production following permafrost thaw. *Nat. Clim. Change* **3**, 890–894 (2013).
29. Miner, K. R. et al. Permafrost carbon emissions in a changing Arctic. *Nat. Rev. Earth Environ.* **3**, 55–67 (2022).
30. Turetsky, M. R. et al. Carbon release through abrupt permafrost thaw. *Nat. Geosci.* **13**, 138–143 (2020).
31. Patzner, M. S. et al. Iron mineral dissolution releases iron and associated organic carbon during permafrost thaw. *Nat. Commun.* **11**, 6329 (2020).
32. Prairie, A. M., King, A. E. & Cotrufo, M. F. Restoring particulate and mineral-associated organic carbon through regenerative agriculture. *Proc. Natl Acad. Sci. USA* **120**, 2217481120 (2023).
33. Ping, C. L. et al. High stocks of soil organic carbon in the North American Arctic region. *Nat. Geosci.* **1**, 615–619 (2008).
34. Mishra, U. et al. Spatial heterogeneity and environmental predictors of permafrost region soil organic carbon stocks. *Sci. Adv.* **7**, eaaz5236 (2021).
35. Ping, C. L., Jastrow, J. D., Jorgenson, M. T., Michaelson, G. J. & Shur, Y. L. Permafrost soils and carbon cycling. *Soil* **1**, 147–171 (2015).
36. Hassink, J. The capacity of soils to preserve organic C and N by their association with clay and silt particles. *Plant Soil* **191**, 77–87 (1997).
37. Cotrufo, M. F. & Lavallee, J. M. Soil organic matter formation, persistence, and functioning: a synthesis of current understanding to inform its conservation and regeneration. *Adv. Agron.* **172**, 1–66 (2022).
38. Prater, I. et al. From fibrous plant residues to mineral-associated organic carbon—the fate of organic matter in Arctic permafrost soils. *Biogeoosciences* **17**, 3367–3383 (2020).
39. Rocci, K. S., Lavallee, J. M., Stewart, C. E. & Cotrufo, M. F. Soil organic carbon response to global environmental change depends on its distribution between mineral-associated and particulate organic matter: a meta-analysis. *Sci. Total Environ.* **793**, 148569 (2021).
40. Allison, S. D., Wallenstein, M. D. & Bradford, M. A. Soil-carbon response to warming dependent on microbial physiology. *Nat. Geosci.* **3**, 336–340 (2010).
41. Liu, F. et al. Altered microbial structure and function after thermokarst formation. *Glob. Change Biol.* **27**, 823–835 (2021).
42. Abbott, B. W. et al. Biomass offsets little or none of permafrost carbon release from soils, streams, and wildfire: an expert assessment. *Environ. Res. Lett.* **11**, 034014 (2016).

**Publisher's note** Springer Nature remains neutral with regard to jurisdictional claims in published maps and institutional affiliations.

Springer Nature or its licensor (e.g. a society or other partner) holds exclusive rights to this article under a publishing agreement with the author(s) or other rightsholder(s); author self-archiving of the accepted manuscript version of this article is solely governed by the terms of such publishing agreement and applicable law.

## Methods

The soil profile in cold regions typically consists of a surface organic horizon (O) overlaying different layers of top- and subsoil mineral horizons (A, B and C)<sup>35</sup>. Considering that the mineral horizon contains the largest amount of SOC in cold regions<sup>34,43</sup>, with the exception of deep Yedoma sediments<sup>44</sup>, and that the organic horizon is dominated exclusively by POC in the form of moderately decomposed plant material<sup>18,38</sup>, we restricted our POC versus MAOC comparison to the mineral layer.

### Meta-analysis of the distribution of SOC fractions in cold systems

We synthesized studies that measured SOC, POC and MAOC concentrations ( $\text{gC kg}^{-1}$  soil<sup>-1</sup>) in the soil mineral layer of terrestrial ecosystems from cold regions (Arctic, subarctic and alpine biomes following the Köppen–Geiger climate classification; Extended Data Fig. 1). The organic layer was not included in our study, and thereby soil C data come exclusively from the mineral layer, independently of the presence or not of the organic layer in the study site. We selected paired observations of POC and MAOC at each site.

A literature search was conducted on 4 May 2022 in the ISI (Institute for Science Information) Web of Knowledge with no restriction on publication year using the following term combinations: (soil carbon or soil organic carbon) and (fraction\* or POM or MAOM or mineral or particulate or physical protection or light fraction\* or macroaggreg\* or microaggreg\* or occluded or stabiliz\* or persisten\*) and (boreal or arctic or subarctic or tundra or permafrost or alpine). We screened previous reviews on the topic to check for missing papers<sup>11</sup>. Then we confronted this list with our selection criteria (Extended Data Table 2). Data from two unpublished studies meeting the selection criteria were also included in the database, one performed at the CiPEHR (Carbon in Permafrost Experimental Heating Research) site in Alaska<sup>45</sup> and one from a global network of terrestrial ecosystems. Studies conducted in Antarctica were removed since soil organic matter formation and turnover are controlled by different factors due to very limited and sparse vegetation. We differentiated between topsoil (the first 30 cm of mineral soil) and subsoil (>30 cm) mineral layers as in recent reviews looking at the global distribution of soil organic matter fractions<sup>11,16</sup>. In essence, an observation was assigned to the topsoil category if sampling in the 0–30 cm depth range and to the subsoil category if sampling at >30 cm soil depth. When multiple depths were sampled within each of our categories, we calculated the depth-weighted mean SOC, POC and MAOC at topsoil and subsoil depths. We finally gathered 37 studies representing 162 observations (Extended Data Fig. 1). See appendix 1 in the Supplementary Information for a list of the articles included in the meta-analysis. The full records of selected articles and the flowchart of preferred reporting items for systematic reviews and meta-analyses (PRISMA) can be found in Extended Data Fig. 6.

Mean, standard deviation and sample size of SOC, POC and MAOC were extracted directly from tables or from graphs using WebPlotDigitizer (<https://automeris.io/WebPlotDigitizer/>). We focused on physical soil organic matter fractionation<sup>10,46</sup>, and included both particle size (MAOC lower than 50–63  $\mu\text{m}$ ) and density (MAOC heavier than 1.60–1.85  $\text{g cm}^{-3}$ ) methods as in recent global analyses<sup>11,16</sup>, because they give very similar results in comparison studies<sup>47</sup> and in their response to environmental variation<sup>39</sup>. The number of observations using the particle size, density and combined size–density were 87, 51 and 24, respectively. When POC and MAOC were split into different components in combined size–density fractionation methods, fractions were summed to total MAOC and POC using SOC concentration and the percentage of each fraction<sup>39</sup>.

We gathered a set of methodological, climate and soil variables from papers and global databases to explore their potential relationships with SOC, POC and MAOC: latitude (54.26° W to 78.73° E), longitude (156.61° S to 177.40° N), MAT (−18.6 to 3.9 °C), MAP (76 to 1,520 mm), biome (Arctic, subarctic or alpine), soil depth

(0 to 126 cm), soil pH (3.29 to 9.10) and soil clay-and-silt content (3.2 to 97.7%). When multiple depths were sampled, we calculated the depth-weighted mean soil properties at surface and subsoil depths. The biome of each site was categorized as Arctic, subarctic or alpine following the Köppen–Geiger climate classification: the average warmest air temperature of any month is below 10 °C at Arctic sites, one to three months average above 10 °C at subarctic sites and one to five months average above 10 °C at alpine sites of the Qinghai-Tibet Plateau. We checked the warmest temperature of any month of the 1900–2019 period using CRUTEM4 accessed through Google Earth<sup>48</sup>. We obtained the mean annual temperature and precipitation of each field study site from the WorldClim v.2.1 database<sup>49</sup>, which provides average climatic values for the period 1970–2000. We used the normalized difference vegetation index (NDVI) from the MODIS (moderate-resolution imaging spectroradiometer) satellite imagery MOD13Q1 product as our proxy of NPP as multiple studies have suggested the existence of a positive relationship between NDVI derived from satellite data and either biomass or annual above-ground NPP for different geographic areas and ecosystems<sup>50</sup>. We followed the standard procedure for NDVI calculation at a global scale<sup>51</sup>. We acquired 23 NDVI values per year with a pixel size of 250 × 250 m and used them to calculate annual NDVI data for each year in the period from 2000 to 2021. To do so, we averaged the product values between the date of the minimum NDVI ( $n$ ) and the date  $n - 1$  of the following year at each site. MODIS data are geometrically and atmospherically corrected and include a reliability index of data quality based on the environmental conditions in which the data were recorded and ranging from 0 (good-quality data) to 4 (raw or absent data). When pixel reliability values were higher than 1, and to avoid using poor-quality data such as pixels covered by snow, NDVI data were discarded.

When not reported in papers, we extracted soil pH and sand content from SoilGrid 2.0 (<https://soilgrids.org/>). We also specified whether the site has active permafrost soil or not. If yes, we recorded the thickness of the active layer (in centimetres) to assess as a surrogate of warming-induced permafrost thaw<sup>27,28</sup>. Gaps in data on the active layer of permafrost sites were filled either with published papers from the same site or using data from the Permafrost Climate Change Initiative<sup>52</sup>.

### Meta-analysis of experimental warming effects on soil carbon fractions in cold systems versus other biomes

We synthesized studies that evaluated the effects of climate warming on SOC, POC and MAOC concentrations ( $\text{gC kg}^{-1}$  soil) in the mineral layer using pairwise field comparisons located side by side under the same climatic and soil conditions. A literature search was conducted on 4 May 2022 in the ISI Web of Knowledge with no restriction on publication year using the following term combinations: (soil carbon) and (fraction\* or POM or MAOM or mineral or particulate or physical protection or light fraction\* or macroaggreg\* or microaggreg\* or occluded or stabiliz\* or persisten\*) and (warming or elevated temperature\*). We screened published reviews to check completeness of our literature compilation<sup>39</sup>. Then we confronted this list with our selection criteria (Extended Data Table 2). Data from one unpublished study performed at the CiPEHR site in Alaska<sup>45</sup> meeting the selection criteria were also included in the database. We finally gathered 20 articles representing 40 observations. See appendix 2 in the Supplementary Information for a list of the articles included in the meta-analysis. The full records of selected articles and the flowchart of PRISMA can be found in Extended Data Fig. 7.

Mean, standard deviation and sample size of SOC, POC and MAOC at control (ambient temperature) and warming (elevated temperature) plots were extracted directly from tables or from graphs using WebPlotDigitizer (<https://automeris.io/WebPlotDigitizer/>). The number of observations using the particle size, density and combined size–density were 8, 15 and 15, respectively. Climate warming treatments included open-top chambers, infrared heaters, heating

cables, geothermal and altitudinal transplants. The biome of each site was categorized as cold system (Arctic, subarctic and alpine) or other (rest of biomes) following the Köppen–Geiger climate classification. We focused our analyses on the first 30 cm of mineral soil as the number of studies including subsoil (>30 cm) measurements was very low. When multiple surface depths were sampled, we calculated the depth-weighted mean SOC, POC and MAOC. Besides biome, we did not explore any other biotic, abiotic or methodological variables as these have been comprehensively tested in ref. 39 and are not necessary to address our very specific research question (does POC respond more strongly to warming in cold systems compared with other biomes?) given the ‘pairing’ of control and treatment plots across potential confounding variables.

## Data analyses

The POC and MAOC concentrations in the top mineral layer (the first 30 cm of mineral soil) and subsoil (>30 cm) layers, and in the topsoil mineral layer of permafrost and non-permafrost soils, and in Arctic, subarctic and alpine biomes did not exhibit normal distributions (Fig. 1). For this reason, POC and MAOC concentrations were first compared using non-parametric paired Wilcoxon signed-rank tests. Then we used parametric linear mixed-effects modelling on natural-log transformed C concentrations to provide support for the Wilcoxon tests and to control for the effects of climate, NPP and soil properties, as well as to account for the lack of independence between observations. In particular, we built a model with a fixed-effects term that included C fraction as a binary variable (POC or MAOC, 1 or 0), together with its interaction with soil depth (topsoil versus subsoil), permafrost (permafrost versus non-permafrost) and biome type (Arctic, subarctic or alpine), as well as MAT, MAP, NPP, soil pH and clay-and-silt content as covariates. In the random term of the model, we used an intercept structure with study plot nested within study to account for the dependence between observations of different depths within the same plot and within the same study.

We also used linear mixed-effects modelling to compare the relative effect sizes of the potential environmental drivers (MAT, MAP, NPP, soil pH and soil clay-and-silt content) on the concentration of each C fraction (POC and MAOC) in the first 30 cm of mineral soil. Spatial associations between observations within the same plot and within the same study were accounted for by random intercept structures in the mixed-effects models. For linear mixed-effects modelling, all numeric variables were standardized by subtracting the mean and dividing by two standard deviations, and binary variables were rescaled to -0.5 and 0.5 (ref. 53). The coefficients and 95% CIs of the models were computed by the restricted maximum likelihood method and bootstrapping (1,000 simulations), and *P* values were estimated on the basis of Satterthwaite approximation. Variance inflation factors (VIFs) and generalized VIFs were calculated to check that the degree of multicollinearity was low (VIF < 2 and generalized VIF < 2.2 for all predictors).

To build confidence in our analysis of the potential environmental controls on POC and MAOC concentrations in the first 30 cm of mineral soil, we also ran random forest modelling. These models are based on the construction of regression trees on bootstrap samples (resampling data allowing for replacement) grown with a subset of predictors. The excluded ‘out-of-bag’ samples are then used to calculate an unbiased error rate, which is essentially a cross-validated error estimate and, thus, eliminates the need for an aside test set<sup>54,55</sup>. Random forests measure relative importance regarding how much each predictor contributes to increasing model accuracy<sup>54</sup>, here computed as the difference in mean-squared error when a variable is held out-of-bag. Variance explained ( $R^2$ ) was calculated by dividing mean-squared error by the variance of the original observations and then subtracting this from one<sup>56</sup>. Although both analyses query data for different purposes (mixed-effects models estimate effect sizes, whereas random forests

explain variation in the outcome), we reasoned that confidence in our analysis of this compiled observational dataset would increase if two contrasting approaches led to similar conclusions.

Wilcoxon signed-rank tests, linear mixed-effects modelling and random forest analyses were carried out using R version 4.1.1<sup>57</sup> and the car<sup>58</sup>, lme4<sup>59</sup>, lmerTest<sup>60</sup>, partR2<sup>61</sup> and randomForest v.4.7-1.1<sup>56</sup> packages.

We explored whether anthropogenic experimental warming affected SOC, MAOC and POC concentrations compared with control plots in cold regions and in other biomes using the log response ratio (RR) as the measure of effect size. The RR is a unit-free index that ranges from  $-\infty$  to  $+\infty$  and estimates the size of the impact and its direction. The RR is calculated as  $\ln(X_w) - \ln(X_c)$ , where  $X_w$  and  $X_c$  are the SOC, MAOC or POC in the warming and control plots, respectively. Zero RR values mean no difference between warming and control plots, and positive and negative values indicate higher and lower SOC, MAOC and POC in warming than in control plots, respectively. For the sake of data interpretation, the RR was converted into the mean percentage of change, being estimated as  $(e^{RR} - 1) \times 100\%$ .

To test whether RR significantly differed from zero, we assessed whether its 95% CI overlapped zero using the open-source software OpenMEE<sup>62</sup>. Specifically, we tested whether the ‘biome type’ of the study (cold systems including Arctic, subarctic and alpine versus other biomes) influenced the effect sizes using weighted random-effects models and a restricted maximum likelihood estimation method. As several studies contributed more than one RR when multiple sites were considered, the variable ‘study’ was included as a random factor in the mixed-effect model. We explored the moderating effect of the categorical covariate ‘biome type’ on the RR using a meta-regression and an omnibus test<sup>62</sup>. The publication bias was assessed with Spearman’s rank correlation tests to analyse the relationships between the effect size and the variance and sample size across studies. The effect sizes of SOC, MAOC and POC were not correlated with data variances or sample sizes ( $P > 0.05$  in all cases).

## Data availability

Data used in this study can be found in the Figshare data repository: <https://doi.org/10.6084/m9.figshare.22347175> (ref. 63).

## Code availability

The code to carry out the current analyses is available from the corresponding author upon request.

## References

43. Tamocai, C. et al. Soil organic carbon pools in the northern circumpolar permafrost region. *Glob. Biogeochem. Cycles* **23**, GB2023 (2009).
44. Strauss, J. et al. Deep Yedoma permafrost: a synthesis of depositional characteristics and carbon vulnerability. *Earth Sci. Rev.* **172**, 75–86 (2017).
45. Plaza, C. et al. Direct observation of permafrost degradation and rapid soil carbon loss in tundra. *Nat. Geosci.* **12**, 627–631 (2019).
46. Golchin, A., Oades, J. M., Skjemstad, J. O. & Clarke, P. Soil structure and carbon cycling. *Aust. J. Soil Res.* **32**, 1043–1068 (1994).
47. Poeplau, C. et al. Isolating organic carbon fractions with varying turnover rates in temperate agricultural soils—a comprehensive method comparison. *Soil Biol. Biochem.* **125**, 10–26 (2018).
48. Harris, I., Osborn, T. J., Jones, P. & Lister, D. Version 4 of the CRUTS monthly high-resolution gridded multivariate climate dataset. *Sci. Data* **7**, 109 (2020).
49. Fick, S. E. & Hijmans, R. J. WorldClim 2: new 1-km spatial resolution climate surfaces for global land areas. *Int. J. Climatol.* **37**, 4302–4315 (2017).

50. Bastos, A., Running, S. W., Gouveia, C. & Trigo, R. M. The global NPP dependence on ENSO: La Niña and the extraordinary year of 2011. *J. Geophys. Res. Biogeosci.* **118**, 1247–1255 (2013).
51. Justice, C. et al. An overview of MODIS Land data processing and product status. *Remote Sens. Environ.* **83**, 3–15 (2002).
52. Obu, J. et al. *ESA Permafrost Climate Change Initiative (Permafrost\_cci): Permafrost Version 2 Data Products* (Centre for Environmental Data Analysis, 2022); <http://catalogue.ceda.ac.uk/uuid/1f88068e86304b0fb34456115b6606f>
53. Gelman, A. Scaling regression inputs by dividing by two standard deviations. *Stat. Med.* **27**, 2865–2873 (2008).
54. Cutler, D. R. et al. Random forests for classification in ecology. *Ecology* **88**, 2783–2792 (2007).
55. Breiman, L. Random forests. *Mach. Learn.* **45**, 5–32 (2001).
56. Liaw, A. & Wiener, M. Classification and regression by randomForest. *R News* **2**, 18–22 (2002).
57. R Core Team R: A Language and Environment for Statistical Computing. Version 4.3.1 (R Foundation for Statistical Computing, 2021); <https://www.R-project.org/>
58. Fox, S. & Weisberg, J. *An R Companion to Applied Regression* 3rd edn (Sage, 2019).
59. Bates, D., Mächler, M., Bolker, B. M. & Walker, S. C. Fitting linear mixed-effects models using lme4. *J. Stat. Softw.* **67** (2015).
60. Kuznetsova, A., Brockhoff, P. B. & Christensen, R. H. B. lmerTest package: tests in linear mixed effects models. *J. Stat. Softw.* **82**, 1–26 (2017).
61. Stoffel, M. A., Nakagawa, S. & Schielzeth, H. partR2: partitioning R2 in generalized linear mixed models. *PeerJ* **9**, e11414 (2021).
62. Wallace, B. C. et al. OpenMEE: intuitive, open-source software for meta-analysis in ecology and evolutionary biology. *Methods Ecol. Evol.* **8**, 941–947 (2016).
63. García-Palacios, P. & Plaza, C. Dominance of particulate organic carbon in top mineral soils in cold regions. *Figshare* <https://doi.org/10.6084/m9.figshare.2234715> (2023).

## Acknowledgements

We thank all authors who gathered and published the raw data in the original studies that enabled this literature synthesis.

P.G.-P. acknowledges support from the Spanish Ministry of Science and Innovation via the I+D+i project PID2020-113021RA-I00 and the TED project TED2021-130908A-C42 (funded by European Union—NextGenerationEU). Work at Lawrence Livermore National Laboratory by N.W.S. was performed under the auspices of the US DOE OBER, under contract DE-AC52-07NA27344 award #SCW1632. M.P. acknowledges financial support by the Comunidad de Madrid and the Spanish National Council of Scientific Researches research grant Atracción de Talento (grant number 2019T1/AMB14503).

## Author contributions

P.G.-P., M.A.B. and C.P. conceived and designed the research, with inputs from N.W.S.; P.G.-P., I.B.-F., J.C.G.-G., A.G.-U., M.P., A.R. and C.P. conducted the literature synthesis. M.D.-B., C.W.M., T.S.-S., E.A.G.S. and L.T. contributed soil samples. P.G.-P., M.d.C., J.J.G. and C.P. conducted the data analyses. The paper was drafted by P.G.-P., and all authors contributed to the final version.

## Competing interests

The authors declare no competing interests.

## Additional information

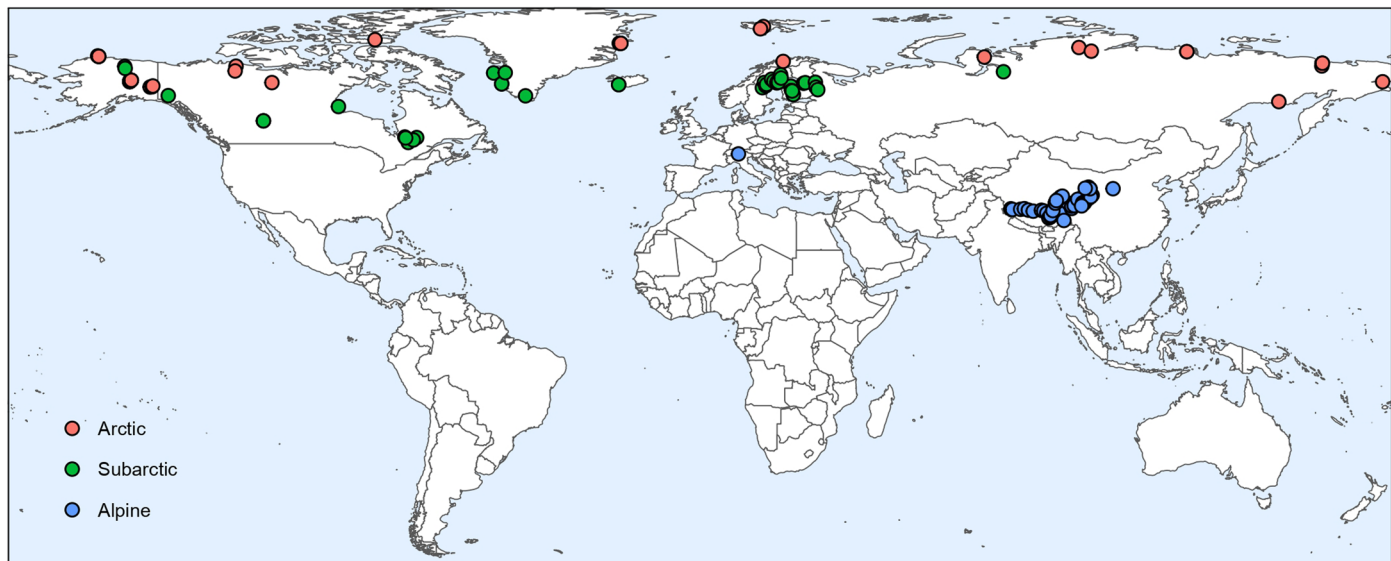
**Extended data** is available for this paper at <https://doi.org/10.1038/s41561-023-01354-5>.

**Supplementary information** The online version contains supplementary material available at <https://doi.org/10.1038/s41561-023-01354-5>.

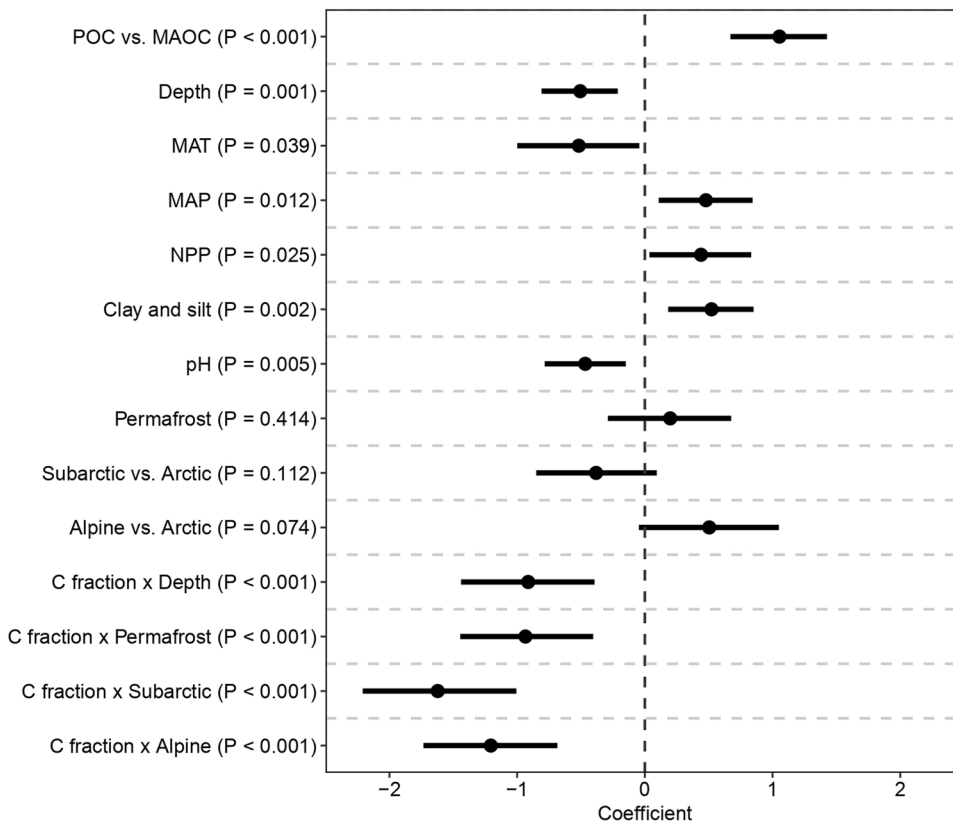
**Correspondence and requests for materials** should be addressed to Pablo García-Palacios.

**Peer review information** *Nature Geoscience* thanks Yuanhe Yang and the other, anonymous, reviewer(s) for their contribution to the peer review of this work. Primary Handling Editor: Xujia Jiang, in collaboration with the *Nature Geoscience* team.

**Reprints and permissions information** is available at [www.nature.com/reprints](http://www.nature.com/reprints).

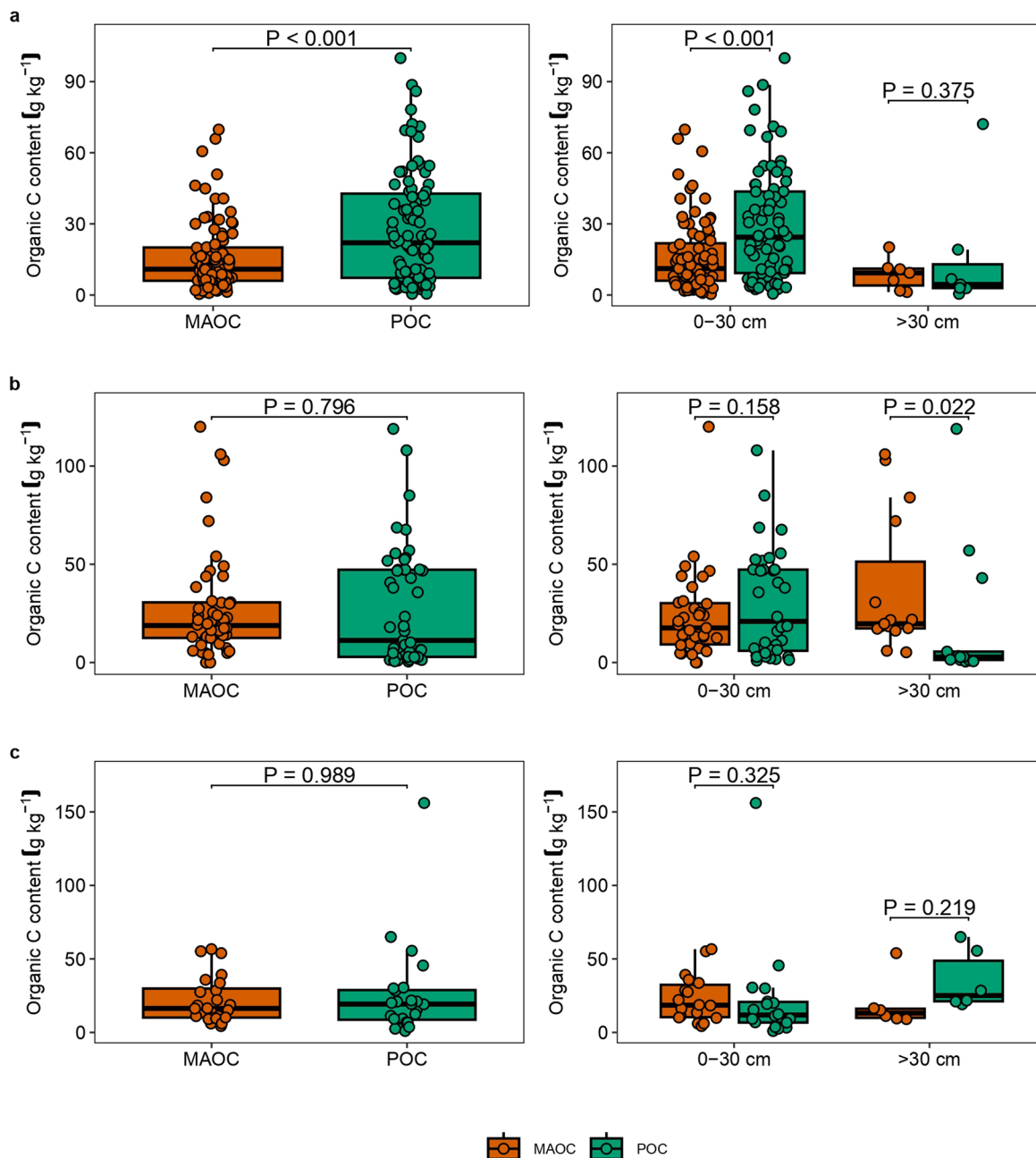


**Extended Data Fig. 1 | Global distribution of the study sites.** Global distribution of the study sites included in the observational meta-analysis addressing the distribution of soil organic carbon in particulate (POC) and mineral-associated (MAOC) fractions in cold systems ( $n=134$ ).


**Extended Data Fig. 2 | Linear mixed-effects modelling on POC and MAOC.**

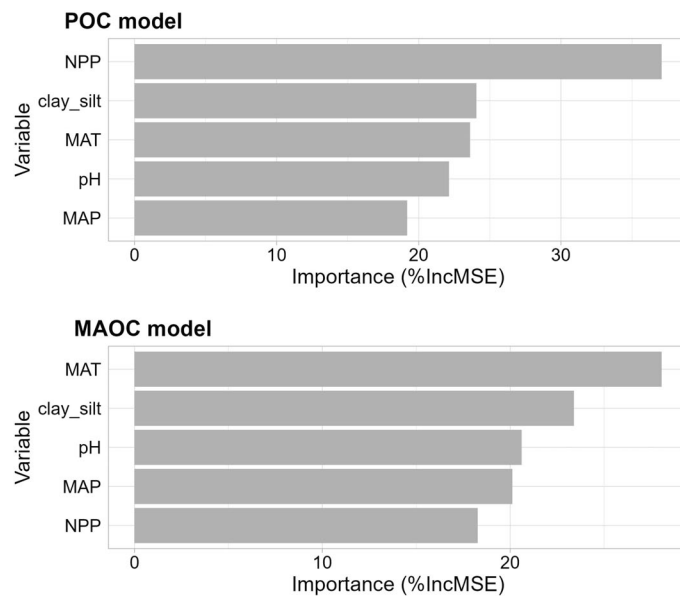
Difference in soil organic carbon concentration in POC vs. MAOC in the mineral layer of cold regions and its interactions with soil depth, permafrost, and biome type (Arctic, Subarctic, and Alpine). Main and interactions effects of C fraction (POC vs. MAOC) controlling for climate (MAT and MAP), net primary productivity (NPP), and soil properties (pH and clay + silt %). The variance explained by the fixed effect predictors and random effects relative to the total variance

( $R^2$ ) was 33% and 12%, respectively ( $n = 309$ ). C fraction concentrations were natural-logarithm transformed. Dots and lines represent coefficients and 95% confidence intervals in the linear mixed effects model with C fraction (POC vs. MAOC) as a binary variable. MAT, mean annual temperature; MAP, mean annual precipitation. The panel corresponds to the first 30 cm of mineral soil.  $P$  values for two-tailed tests.



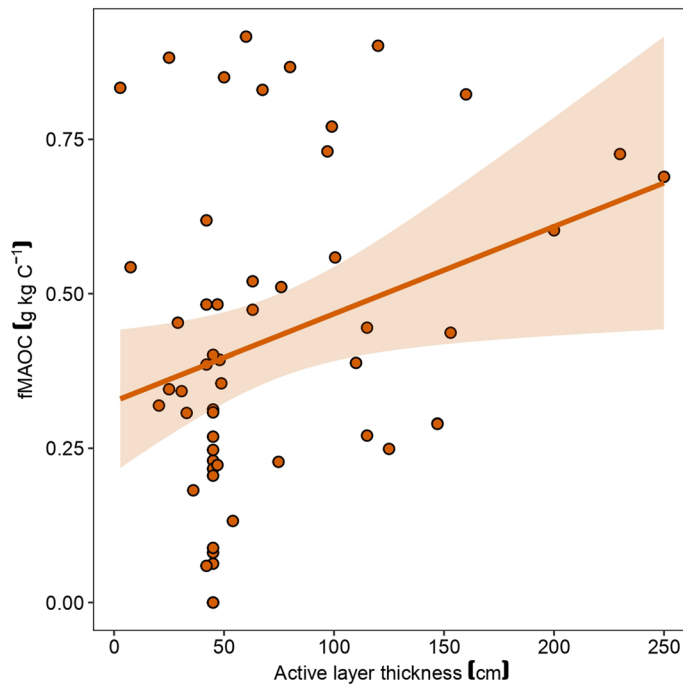
**Extended Data Fig. 3 | POC and MAOC by fractionation method.** Distribution of soil organic carbon in the POC and MAOC fractions in the mineral layer of cold regions separated by (a) size, (b) density, and (c) combination of size and density methods. Panels represent (left) overall fraction distribution or separated by (right) soil depth. Results from paired Wilcoxon signed-rank tests. POC = particulate organic C; MAOC = mineral-associated organic C. Box plots represent

1st and 3rd quartiles (box), medians (central horizontal line), largest value smaller than 1.5 times the interquartile range (upper vertical line), and smallest value larger than 1.5 times the interquartile range (lower vertical line). n = 87, 48 and 24 for both fractions in a, b and c, respectively. n = 80, 35 and 18 in a, b and c, respectively, in the first 30 cm of mineral soil. n = 7, 13 and 5 in a, b and c, respectively, in >30 cm. P values for two-tailed tests.

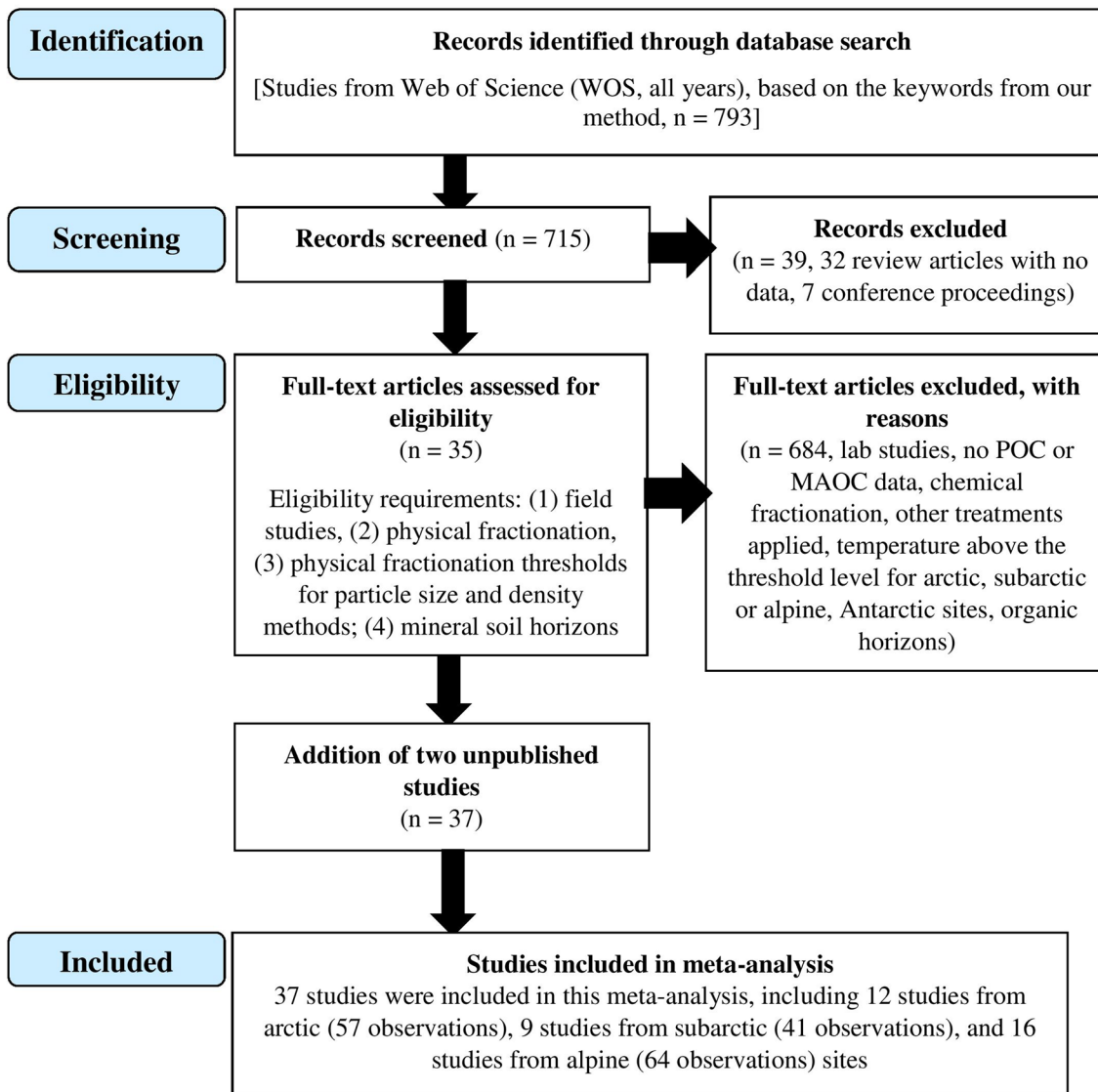


**Extended Data Fig. 4 | Random forest: environmental drivers versus POC and MAOC.** Random forest analysis to identify the relative importance of the different environmental drivers predicting soil organic carbon concentration in POC vs. MAOC in the mineral layer of cold regions. The relative importance

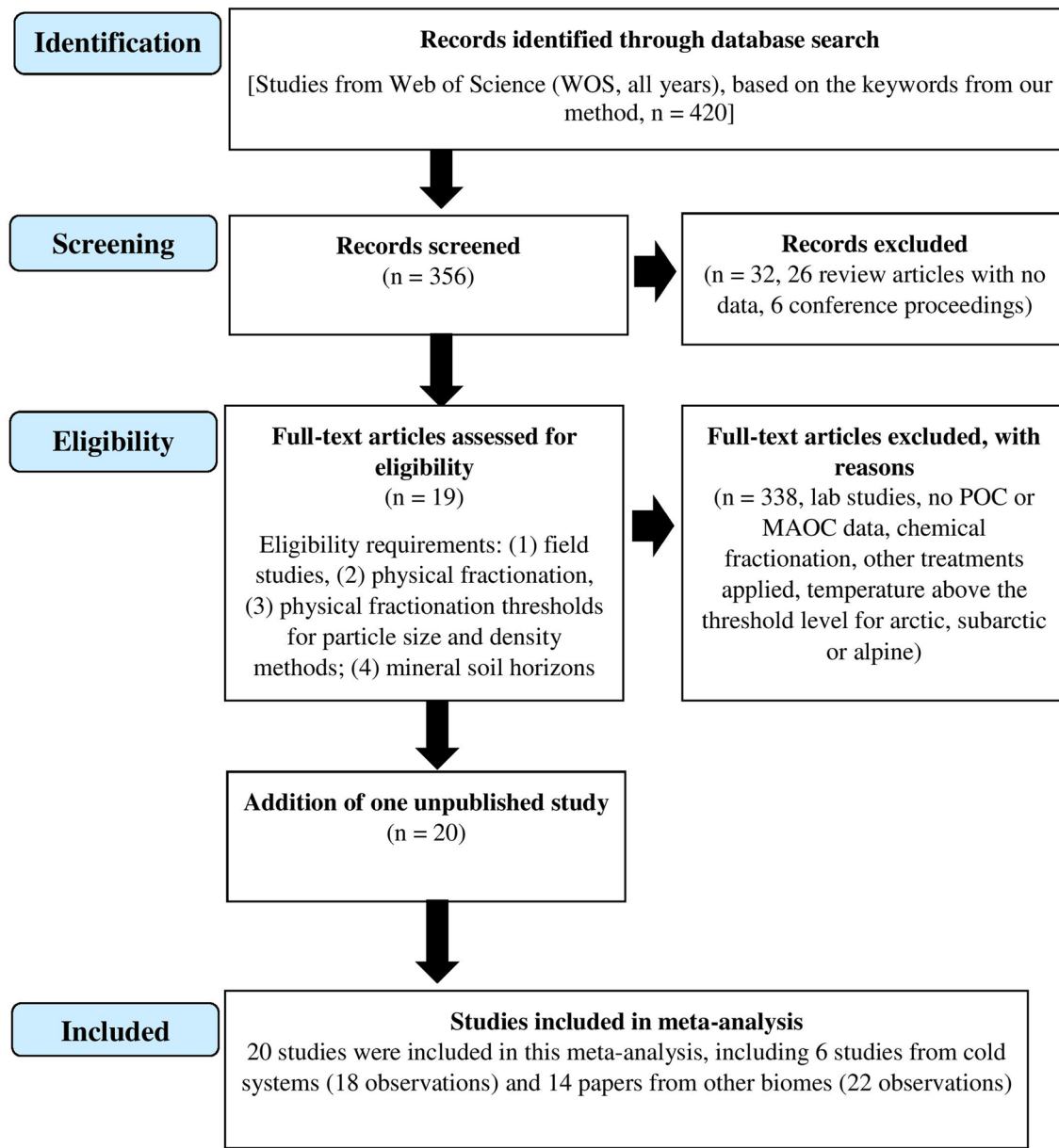
is estimated on the basis of the increase in mean-square error (%IncMSE). This analysis was performed using data from the first 30 cm of mineral soil. POC random forest:  $R^2 = 0.45$  and  $MSE = 0.762$  ( $n = 128$ ), MAOC random forest:  $R^2 = 0.36$  and  $MSE = 0.519$  ( $n = 127$ ).



**Extended Data Fig. 5 | Active layer thickness versus fMAOC.** Relationship between active layer thickness and proportion of MAOC relative to SOC (fMAOC). Line and shading represent linear regression and 95% confidence intervals ( $f\text{MAOC} = 0.33 + 0.0014 \times \text{Active layer thickness}$ ,  $n = 133$ ,  $R^2 = 0.09$ ,  $P = 0.031$ ). The panel corresponds to the first 30 cm of mineral soil.



**Extended Data Fig. 6 | PRISMA-flowchart: observational meta-analysis.** PRISMA-flowchart of assessment of eligible studies in the observational meta-analysis of soil carbon fractions distribution in cold systems.



**Extended Data Fig. 7 | PRISMA-flowchart: experimental meta-analysis.** PRISMA-flowchart of assessment of eligible studies in the meta-analysis of experimental warming effects on soil carbon fractions.

**Extended Data Table 1 | Random-effects models of experimental warming**

Moderator	Levels	n	Fraction	Effect Size	Lower Confidence Interval	Upper Confidence Interval
Biome	Cold	18	SOC	-15.465	-30.163	2.327
	Other	22	SOC	-0.300	-13.151	14.454
Biome	Cold	18	MAOC	-5.541	-17.139	7.681
	Other	22	MAOC	-0.399	-12.628	13.655
Biome	Cold	18	POC	-27.892	-47.481	-0.896
	Other	22	POC	17.000	-4.400	43.333

Results of the weighted random-effects models performed on experimental field studies comparing the first 30 cm of mineral soil in warming and ambient temperature plots in cold systems versus other biomes.

## Extended Data Table 2 | Study selection criteria

Meta-analysis	Selection criteria
Obs & Exp	In order to conduct a weighted meta-analysis <sup>1</sup> , we limited our data collection to studies in which means, standard deviations and replicate numbers were reported or could be determined. When suitable studies lacked information, or we could not retrieve it, the authors were contacted and asked for their original data.
Obs & Exp	When the same article reported results from more than one study system (e.g. different geographical location, warming level, parent material, ecosystem, microclimate or dominant vegetation), we considered each of these separately, as they represented different examples of climate warming effects on SOM fractions <sup>2,3</sup> (e.g. García-Palacios et al. 2015; Song et al. 2019). While strictly speaking results from different plant species/sites within each study are not independent, we retained them as separate observations to ensure that the results of our analyses were as general as possible. Although this approach tends to reduce the overall heterogeneity in effect sizes, excluding multiple results from one data source can underestimate effect sizes <sup>1,4</sup> .
Exp	The control (ambient temperatures) and treatment (warming temperatures) plots were located in the same site (except for altitudinal transplants). This allowed us to be certain that any difference observed at each observation could be attributed to the effects of warming, and not to variations in microclimate or soil type between treatments. If the study manipulated other factors (e.g. nutrients, drought, vegetation removal, farming practices), only results from non-manipulated plots were considered.
Exp	Only field studies were selected.
Obs & Exp	When SOM fractions were measured at multiple sampling dates, only the latest sampling date was included in the analysis.
Exp	In some cases, more than one paper reported data from a particular experiment. We reported only data from the study covering the longest period
Obs & Exp	We only focused on physical fractionation methods such as particle size and density. Chemical fractionation methods (stepwise hydrolysis, H <sub>2</sub> O <sub>2</sub> , Na <sub>2</sub> S <sub>2</sub> O <sub>8</sub> , NaOCl, NaOCl + HF) were excluded.

Study selection criteria. Observational meta-analysis of soil carbon fractions distribution in cold systems (Obs). Experimental meta-analysis of warming effects on soil carbon fractions in cold systems vs. other biomes (Exp). See Appendix S3 for cited references.